http://dx.doi.org/10.14500/aro.11522

Synthesis Development and Molecular Docking Study of New Azo Chalcone Derivatives

Myasar Kh. Ibrahim[1†] and Shireen R. Mohammed[2]

[1]Department of Basic Science, College of Agricultural Engineering Sciences, University of Duhok, Duhok, Kurdistan Region – F.R. Iraq

[2]Department of Chemistry, College of Science, University of Zakho, Duhok, Kurdistan Region – F.R. Iraq

***Abstract*—This work is divided into two main parts. The first part involves the synthesis of new azo chalcone compounds through a two-step process. Initially, azo compounds are synthesized by diazotizing 3-nitroaniline, followed by a coupling reaction with 4-hydroxyacetophenone, which has a terminal ketone group. Subsequently, the resulting product undergoes a Claisen–Schmidt condensation reaction with various aromatic aldehyde substrates to produce new α, β-unsaturated ketones, known as azo chalcone compounds. The successful synthesis of these compounds is confirmed using Fourier-transform infrared spectroscopy, ^{1}H NMR, and ^{13}C NMR spectral analyses. The second part of this study explores the theoretical biological activity of the synthesized compounds against severe acute respiratory syndrome coronavirus 2 through molecular docking studies. The results indicate potential antiviral properties for each compound, with compounds B5 and B8 exhibiting the most promising results. These compounds achieved higher docking scores (ΔG −6.235 kcal/mol and −5.832 kcal/mol, respectively) and each formed four hydrogen bonds with the target protein.**

***Index Terms*—Antiviral activity, Azo chalcone compounds, Molecular docking, Severe acute respiratory syndrome coronavirus 2, Synthesis.**

I. Introduction

Azo chalcone compounds contain two significant functional groups: (-CH=CHCO-) and (-N=N-) and have two isomers, *trans* and *cis*; the *trans* isomer is more common. Therefore, they are widely used for dying in industries (Vollheim, 1993), the final product in pharmaceuticals (Mezgebe and Mulugeta, 2022), and they have biological activity such as anticancer "antitumor breast cancer cells" (Baper and Mohammd, 2023), antimicrobial "against *Staphylococcus aureus* and *Bacillus subtilis*", and antioxidant "Ferrous ion-chelating activity" (Okolo, et al., 2021; Rohini, Devi and Devi, 2015). Different modifications and routes are made to obtain azo chalcones with desired properties (Kadhium, Mohammed and Baper, 2023; ALKazmi, Hawais and Alasadi, 2023; Baper and Mohammd, 2023). The most common synthesis method for preparing azo compounds is amine diazotization, which was reported first by the German organic chemist Peter Griess in 1858 (Yates and Yates, 2016). The diazotization consists of nitrosation of primary aromatic amines with nitrous acid to produce diazonium salts then coupling with nucleophiles such as *ortho*- or *para*-phenol or aniline. These compounds can be identified by their functional group (–N=N–), which has particular interest due to their strong bioactivities (Yates and Yates, 2016; Abbas, Al-Hamdani and Shaker, 2011), such as antimicrobial (Gür, 2019; Kofie, Dzidzoramengor and Adosraku, 2015), anti-bacterial (Mamand, et al., 2024), anti-fungal (Mezgebe and Mulugeta, 2022), anti-inflammatory (Mamand, et al., 2024), anti-viral (Mezgebe and Mulugeta, 2022), and anti-tubercular and anti-cancer (Kofie, Dzidzoramengor and Adosraku, 2015). Furthermore, azo compounds are used in pharmacological applications (Mezgebe and Mulugeta, 2022) such as HIV inhibitors of viral replication, including Evans blue and Congo red (Kozlowski and Watson, 1992). It is thought that the binding of azo dyes to this virus's reverse transcriptase and protease is what causes this effect. Various compounds have demonstrated antibacterial and pesticidal properties due to the presence of an azo moiety (Katritzky, Chen and Tala, 2009; Hawaiz and Samad, 2012); azo-imine (Hussein and Aziz, 2011); azo-pyrazoline derivatives (Hawaiz, Hussein and Samad, 2014); pyrimidine derivatives (Mamand, et al., 2024); moreover, azo compounds were used as dyes more than half of all commercial colorants (Benkhaya, M'rabet and El Harfi, 2020). Azo benzene derivatives with active functional groups such as formyl or acetyl groups are produced by the most significant reaction, azo linkage, which links highly activated aromatic rings through an electrophilic aromatic substitution reaction. For these reasons, azo-compounds have huge literature publications.

Claisen–Schmidt condensation reaction (crossed-aldol reaction) is a powerful tool for the synthesis α,β-unsaturated ketones (chalcones) which have a general formula C_6H_5CH=CHCOPh. Acetophenone and benzaldehyde, or their

ARO-The Scientific Journal of Koya University
Vol. XII, No. 2 (2024), Article ID: ARO.11522. 9 pages
DOI: 10.14500/aro.11522
Received: 17 January 2024; Accepted: 02 August 2024
Regular research paper: Published: 18 August 2024
†Corresponding author's e-mail: myasar.ibrahim@uod.ac

modified form, can undergo this reaction in the occurrences of sodium hydroxide in ethanol to produce chalcone (Kaka, Dabbagh and Hamad, 2016; Calvino, et al., 2005; Hsieh, et al., 2012; Aksöz and Ertan, 2012). Furthermore, the azo compound that contains terminal ketone reacts with different aromatic aldehyde substrates through Claisen–Schmidt condensation to obtain chalcones attached to an azo compound called azo chalcone compounds (ALKazmi, Hawais and Alasadi, 2023; Hawaiz, Samad and Aziz, 2015). This process involves the formation of a carbon–carbon new bond and holds great significance in the field of organic synthesis (Zweifel, Nantz and Somfai, 2017). Chalcone compounds have several different names such as methyl styryl ketone (Sivasankerreddy, et al., 2018) and benzylideneacetophenone benzalacetone (Tawfiq, 2016). Because chalcone derivatives have a ketoethylenic moiety (CO−CH=CH−), they are a valued species (Elkanzi, et al., 2022).

Our current work builds upon our ongoing efforts to design, synthesize, and identify new molecules derived from azo chalcone. This is achieved through two main processes. First, the reaction between 3-nitroaniline and 4-hydroxyacetophenone takes place under basic conditions in a coupling reaction step. Second, the coupling product is reacted with various aromatic aldehyde substrates under basic conditions using the Claisen–Schmidt condensation protocol. This ultimately yields new azo chalcone products, as shown in Fig. 1.

II. Experimental

A. Materials and Methods

The chemicals and solvents used in this work were purchased from Scharlau, Merck, and Fluka Companies and were used without any further purification. Melting points were measured with an uncorrected measuring device of melting point (melting point type: Electrothermal 12372). Fourier-transform infrared spectra were recorded using Thermo Scientific Nicolet iS 20 Fourier-transform infrared spectroscopy (FT-IR) Spectrometer station (4000–400 cm^{-1}) used for attenuated total reflectance (ATR) vibration measurements with (4 cm^{-1}) resolution. The software Omnic 9.2.86, Firmware version 1.02 by Thermo Fisher Scientific, was used for data collection, drawing, and interpretation of FT-IR (ATR) spectra. NMR spectra were recorded by Bruker NMR spectrometer, operating at (400 MHz) with an internal standard; tetramethylsilane, and all NMR spectra were measured at the Department of Chemistry/College of Education/University of Basra. Preparative thin layer chromatography (TLC) silica gel 60, F254 Glass used for clean-up compounds.

B. Synthesis

Preparation of hydroxy-3-((3nitrophenyl)diazenyl)phenyl.) ethan-1-one (B1)

The compound (**B1**) was synthesized according to the patent (Botros and Creek, 1977), with some development as shown: In a 1 L, 3-Nitroaniline (8.28 g, 60 mmol, 1.0 eq.) was dissolved in 25 mL of distilled water and concentrated hydrochloric acid (HCl) (23 mL), the solution was cool down to 0–5°C in ice-bath with stirring. A cold solution of sodium nitrate (8.28 g, 120 mmol, 2eq.) in 15 mL distilled water was added drop by drop to the content of the flask, stirring for (1 h) while keeping the same temperature. The final cold aqueous mixture in the above flask, which contains the product of diazonium salt, was added dropwise to the basic phenolic solution with stirring in an ice bath for (4 h). The phenolic solution consists of; sodium carbonate (22 g, 207 mmol, 3.45 eq.), distilled water (220 mL) and 4-hydroxy acetophenone (8.209 g, 60.3 mmol, 1.005 eq.). The cold mixture was filtered using Buchner under vacuum; the precipitant was washed with distilled water and acidified with 2N, HCl and filtered, then washed with boiling distilled water twice and followed by purification using preparative TLC to give the expected product as shown in Table I.

General procedure for the synthesis of azo chalcones (B2-B12)

Azo chalcones were prepared from compound (B1) after converting it (B1) to Enolate form, which was prepared by dissolving NaOH (0.6 g, 15 mmol, 4.28eq.) in ethanol (15 mL) then 1 g, 3.5 mmol, 1eq. of azo compound **B1** was added with stirring for 48 h in 28°C. Aromatic aldehyde substrates (5 mmol, 1.4eq.) were dissolved in ethanol (25 mL) and added drop by drop to the Enolate solution, then stirred for (4–48 h), then filtered, acidify by (2M, HCl) and filtered, then washed with boiling distilled water and hot ethanol, to give the expected products as shown in Table I. All monitoring compounds were using TLC and preparative TLC with eluents (toluene/ethyl acetate [EtOAc] 3:1).

C. Molecular Docking Study

Molecular docking is commonly used to detect the best binding direction of a molecule linked to the molecule of a protein to calculate binding energy and predict biological activity depending on ΔG [Kcal/mol] as shown in Table II.

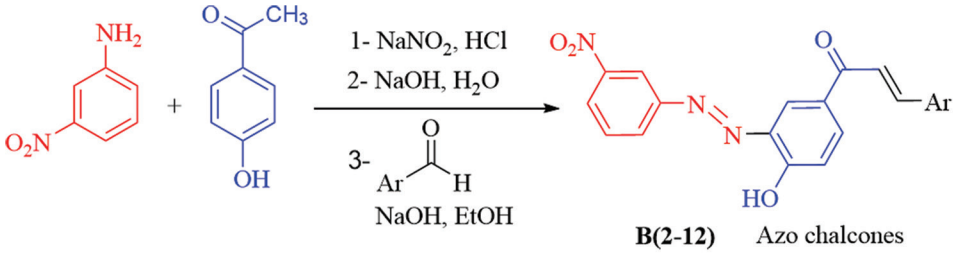

Fig. 1. Synthetic route of azo chalcone products.

 http://dx.doi.org/10.14500/aro.11522

TABLE I
THE PHYSICAL PROPERTIES OF THE SYNTHESIS COMPOUNDS

Compound	- Ar	M.P.	Color	TLC R_f	Yield %
B1		181–184	Brown	0.7	94
B2	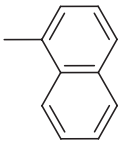	195–196	Brown	0.8	68
B3	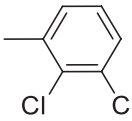	228–229	Yellow	0.85	94
B4	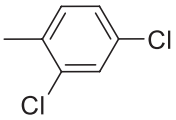	226–227	Yellow	0.83	97
B5	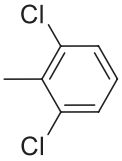	222–223	Yellow	0.82	93
B6	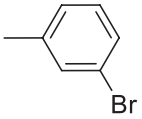	142–145	Dark brown	0.8	68
B7	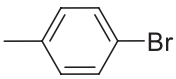	227–228	Light brown	0.75	96
B8	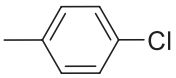	218–220	Brown	0.8	94
B9	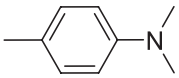	183–185	Brown	0.6	82
B10	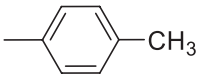	182–184	orange	0.78	95
B11	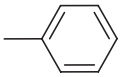	193–194	Light brown	0.7	96
B12	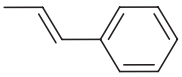	175–177	Brown	0.78	86

TLC: Thin layer chromatography

The template of severe acute respiratory syndrome coronavirus 2 (SARS-CoV-2) 3CL protease was collected from the protein bank which is shown in Fig. 2, before the docking process. Then, setups of 12 different ligands were built in by ChemDraw, and the Chem3D software was used to transform the 2D structure into the 3D structure. Through energy minimization, the best ligand three-dimensional (3D) structure was chosen, to predict the strength of the bond; optimum conformation was chosen and used. The receptor of the virus (SARS-CoV-2 3CL protease) was significantly reduced utilizing protein preparation and reduction techniques from the PyRx libraries, which is a powerful molecular docking tool that is used to find the binding ability lies between the receptor and ligand. A molecular docking program that gives effective docking results (Chawsheen and Al-Bustany, 2019) called AutoDock Vina, PyRx, and PyMol software were used for all newly synthesis compounds **B2-B12** with the crystallographic structure of SARS-CoV-2 as a molecule target Fig. 2. The active site of the receptor SARS-CoV-2 3CL protease contains the amino acid residues shown in Fig. 3a and b.

III. Results and Discussion

Our protocol of the synthesis consists of two general lines; first, preparation of a new azo compound (**B1**) through a diazotization reaction at a low temperature, of 3-nitroaniline with nitrous acid to produce diazonium salts, followed by one-pot coupling the diazonium salt with 4-hydroxyacetophenone in basic ethanolic solution of NaOH. Second, the compound **B1** reacts with various aromatic aldehyde substrates (–Ar) Table I in an ethanolic solution of NaOH at room temperature to produce new azo chalcone compounds **B2-B12**, as shown in Fig. 4. The final expected products were easily isolated through preparative TLC and purification as shown in Fig. 5, giving acceptable yields (68–97%).

The physical properties of the prepared compounds were studied and are shown in Table I.

A. FTIR (ATR) Spectra Measurements

The resulting compounds were identified using FTIR technology, the ATR was used with novel ZnSe crystal to

TABLE II
MOLECULAR DOCKING SCORES FOR THE SYNTHESIS COMPOUNDS

Compound	Name	Docking score (ΔG)
B1	1-(4-hydroxy-3-(((3-nitrophenyl) diazenyl) phenyl) ethan-1-one	−5.54
B2	1-(4-hydroxy-3-(((3-nitrophenyl) diazenyl) phenyl)-3-(naphthalene-1-yl) prop-2-en-1-one	−5.324
B3	3-(2,3-dichlorophenyl)-1-(4-hydroxy-3-(((3-nitrophenyl) diazenyl) phenyl) prop-2-en-1-one	−5.657
B4	3-(2,4-dichlorophenyl)-1-(4-hydroxy-3-(((3-nitrophenyl) diazenyl) phenyl) prop-2-en-1-one	−5.432
B5	3-(2,6-dichlorophenyl)-1-(4-hydroxy-3-(((3-nitrophenyl) diazenyl) phenyl) prop-2-en-1-one	−6.235
B6	3-(3-bromophenyl)-1-(4-hydroxy-3-(((3-nitrophenyl) diazenyl) phenyl) prop-2-en-1-one	−5.823
B7	3-(4-bromophenyl)-1-(4-hydroxy-3-((E)-(3-nitrophenyl) diazenyl) phenyl) prop-2-en-1-one	−5.789
B8	3-(4-chlorophenyl)-1-(4-hydroxy-3-(((3-nitrophenyl) diazenyl) phenyl) prop-2-en-1-one	−5.832
B9	3-(4-(dimethylamino) phenyl)-1-(4-hydroxy-3-((3-nitrophenyl) diazenyl) phenyl) prop-2-en-1-one	−5.456
B10	1-(4-hydroxy-3-(((3-nitrophenyl) diazenyl) phenyl)-3-(p-tolyl) prop-2-en-1-one	−5.654
B11	1-(4-((5-acetyl-2,4-dihydroxyphenyl) diazenyl) phenyl) ethan-1-one	−5.325
B12	1-(4-hydroxy-3-((3-nitrophenyl) diazenyl) phenyl)-5-phenylpenta-2,4-dien-1-one	−5.364

analyze the synthesis compounds, and all results are shown in Table III spectrum of the compounds, the bands that appear at 1600–1670 cm^{-1} are due to stretching (str.) vibration (vib) of carbonyl group (-C=O). The bands at (950–1000) cm^{-1}, (1600–1660) cm^{-1}, and (3060–3085) cm^{-1} belong to str. vib. of (C-H) alkene, aliphatic, and aromatic, respectively. The moderate bands appear at 1250–1335 cm^{-1} and belong to str. vibrations of C-N. The bands at 1350 cm^{-1} and 1530 cm^{-1} belong to (NO_2) str. symmetric and asymmetric vib., respectively. The band that appears at 3100–3320 is attributed to str. vibration of O-H. The band at 1035–1100 cm^{-1} is attributed to C-Cl str. vib. for chloro-substituted compounds (Shriner, et al., 2004; Pretsch, Bühlmann and Badertscher, 2000; Clayden, Greeves and Warren, 1995).

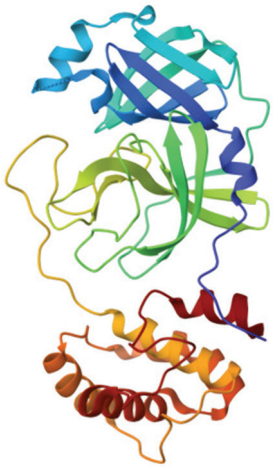

Fig. 2. 3D image severe acute respiratory syndrome coronavirus 2 3CL.

The overlay IR spectrum in Fig. 6 shows the confirmation of producing the **B1** compound by disappearing NH_2 peak from 3-Nitroaniline and appearing N=N and C-N peaks in product **B1**. Furthermore, ATR overlay spectrums in Fig. 7 illustrate the difference between reactant B1 and product B8, which provided evidence of producing azo chalcone compound B8.

B. ^{1}HNMR and ^{13}CNMR Spectrums of Compounds

The ^{1}H NMR spectra of synthesized azo compound **B1** showed the following characteristic chemical shifts (δ), as a singlet at 12.86 ppm for the OH group, singlet at 2.68 ppm for CH3. The ^{13}C NMR appears singlet at 195.89 and 26.52 ppm for C=O and OH groups, respectively. The ^{1}H-NMR spectrum of synthesized azo chalcone compound **B3** is shown in Fig. 8. All ^{1}H-NMR spectra of the synthesized azo compounds showed the following characteristic chemical shifts (δ), the significant doublet peaks of the AB system for each proton of (-HC=CH-) appear in two regions: first at (8.18–7.4) ppm, with J coupling at 15.60 Hz for all compounds except B2 and B6, at 15.20 Hz. While the second peak appeared at (7.94–7.38) with J coupling at 15.60 Hz for all compounds except B2 and B6, it was at 15.20 Hz. This is very important evidence of the formation of the double bond for chalcones. Furthermore, extra peaks at 7.00-8.84 which belong to the aromatic system. The ^{13}C NMR spectrum of synthesized azo

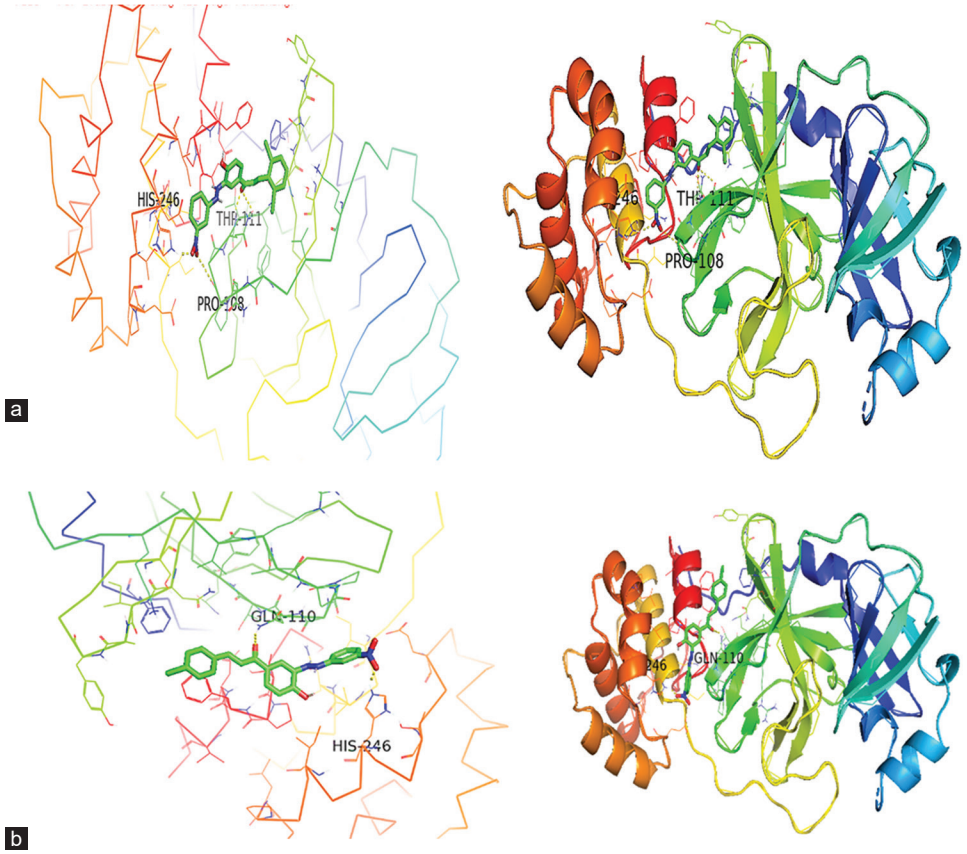

Fig. 3. Binding and docking interaction between severe acute respiratory syndrome coronavirus 2 3CL and compound: (a) **B5,** (b) **B8**.

http://dx.doi.org/10.14500/aro.11522

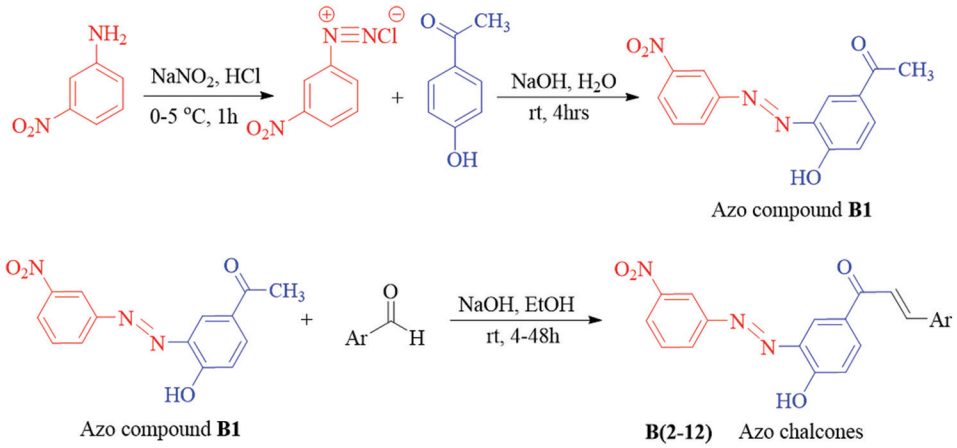

Fig. 4. Synthesis of azo chalcone compounds.

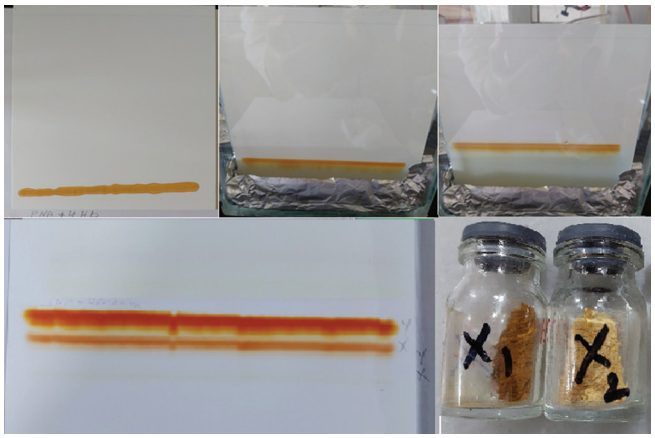

Fig. 5. Purification process of the azo compound using preparative thin-layer chromatography.

chalcone compound **B3** is shown in Fig. 9. The ^{13}C NMR for all synthesized azo compounds appears with two significant peaks at 136–145 ppm and 125.41–125.93 ppm for two carbons of C=C. The following data illustrates ^{1}H NMR interpretation for synthesized compounds.

(**B1**) ^{1}H NMR (400 MHz, $CDCl_3$) δ 12.90 (s, 1H, OH), 8.77 (t, J = 2.4 Hz, 1H, CH_{ar}), 8.73 (d, J = 2.4 Hz, 1H, CH_{ar}), 8.38 (ddd, J = 8.4, 2.4 and 1.2 Hz, 1H, CH_{ar}), 8.25 (ddd, J = 8.0, 2 and 1.2 Hz, 1H, CH_{ar}), 8.19 (dd, J = 8.8 and 2.4 Hz, 1H, CH_{ar}), 7.90 (d, J = 15.6 Hz, 1H, CH=CH), 7.76 (t, J = 8.0 Hz, 1H, CH_{ar}), 7.74–7.7 (m, 2H, CH_{ar}), 7.65 (d, J = 15.6 Hz, 1H, CH=CH), 7.45–7.44 (m, 3H, CH_{ar}), and 7.18 (d, J = 8.8 Hz, 1H, CH_{ar}).

(**B2**) ^{1}H NMR (400 MHz, $CDCl_3$) δ 12.91 (s, 1H, OH), 8.80–8.72 (m, 3H, CH_{ar}), 8.36 (ddd, J = 8.3, 2.4, 1.1 Hz, 1H, CH_{ar}), 8.29 (d, J = 8.4 Hz, 1H, CH_{ar}), 8.23 (dd, J = 8.7, 2.1 Hz, 2H, CH_{ar}), 7.99–7.87 (m, 3H, CH_{ar}), 7.74–7.52 (m, 5H, CH_{ar} and CH=CH), and 7.20 (d, J = 8.8 Hz, 1H, CH_{ar}).

(**B3**) ^{1}H NMR (400 MHz, DMSO) δ 11.68 (s, 1H, OH), 8.79 (t, J = 2.1 Hz, 1H, CH_{ar}), 8.50–8.47 (m, 2H, CH_{ar}), 8.38 (dd, J = 8.2, 2.4 Hz, 1H, CH_{ar}), 8.27 (t, J = 9.1 Hz, 2H, CH_{ar}), 8.02 (d, J = 15.6 Hz, 1H, CH=CH), 7.95–7.87 (m, 2H, CH_{ar} and CH=CH), 7.72 (d, J = 2.2 Hz, 1H, CH_{ar}), 7.53 (dd, J = 8.5, 2.2 Hz, 1H, CH_{ar}), and 7.23 (d, J = 8.7 Hz, 1H, CH_{ar}).

(**B4**) ^{1}H NMR (400 MHz, DMSO) δ 11.71 (s, 1H, OH), 8.81 (t, J = 2.1 Hz, 1H, CH_{ar}), 8.52–8.48 (m, 2H, CH_{ar}), 8.40 (dd, J = 8.2, 2.3 Hz, 1H, CH_{ar}), 8.34–8.26 (m, 2H, CH_{ar}), 8.06 (d, J = 15.6 Hz, 1H, CH=CH), 7.97–7.88 (m, 2H, C_{ar} and CH=CH), 7.74 (d, J = 2.1 Hz, 1H, CH_{ar}), 7.55 (dd, J = 8.5, 2.2 Hz, 1H, CH_{ar}), and 7.24 (d, J = 8.7 Hz, 1H, CH_{ar}).

(**B5**) ^{1}H NMR (400 MHz, DMSO) δ 11.70 (s, 1H, OH), 8.81 (s, 1H, CH_{ar}), 8.51–8.41 (m, 3H, CH_{ar}), 8.20 (d, J = 8.7 Hz, 1H), 7.91 (t, J = 8.0 Hz, 1H, CH_{ar}), 7.81 (d, J = 15.6 Hz, 1H, CH=CH), 7.70–7.6 (m, 3H, CH_{ar} and CH=CH), 7.45 (t, J = 8.4 Hz, 1H, CH_{ar}), and 7.28 (d, J = 8.6 Hz, 1H, CH_{ar}).

(**B6**) ^{1}H NMR (400 MHz, DMSO) δ 11.70 (s, 1H, OH), 8.81 (t, J = 2.1 Hz, 1H, CH_{ar}), 8.51–8.48 (m, 1H, CH_{ar}), 8.39 (dd, J = 8.2, 2.3 Hz, 1H, CH_{ar}), 8.30 (dd, J = 8.6, 2.3 Hz, 1H, CH_{ar}), 8.22 (d, J = 7.8 Hz, 1H, CH_{ar}), 7.99–7.88 (m, 4H, CH_{ar}), 7.73 (d, J = 8.0 Hz, 1H, CH_{ar}), 7.49 (t, J = 7.5 Hz, 1H, C=C), 7.41–7.35 (m, 1H, C=C), and 7.25 (d, J = 8.6 Hz, 1H, CH_{ar}).

(**B7**) ^{1}H NMR (400 MHz, DMSO) δ 11.65 (s, 1H, OH), 8.81 (t, J = 2.1 Hz, 1H, CH_{ar}), 8.52–8.47 (m, 2H, CH_{ar}), 8.39 (dd, J = 8.3, 2.3 Hz, 1H, CH_{ar}), 8.30 (dd, J = 8.7, 2.3 Hz, 1H, CH_{ar}), 7.99 (d, J = 15.5 Hz, 1H, CH=CH), 7.95–7.85 (m, 3H, CH_{ar}), 7.72 (d, J = 15.5 Hz, 1H, CH=CH), 7.52 (d, J = 8.4 Hz, 2H, CH_{ar}), and 7.24 (d, J = 8.7 Hz, 1H, CH_{ar}).

(**B8**) ^{1}H NMR (400 MHz, DMSO) δ 11.66 (s, 1H, OH), 8.84 (t, J = 2.0 Hz, 1H, CH_{ar}), 8.54–8.49 (m, 2H, CH_{ar}), 8.41 (dd, J = 8.1, 2.3 Hz, 1H, CH_{ar}), 8.32 (dd, J = 8.7, 2.2 Hz, 1H, CH_{ar}), 8.02 (d, J = 15.6 Hz, 1H, CH=CH), 7.97–7.9 (m, 3H, CH_{ar}), 7.75 (d, J = 15.5 Hz, 1H, CH=CH), 7.54 (d, J = 8.1 Hz, 2H, CH_{ar}), and 7.26 (d, J = 8.7 Hz, 1H, CH_{ar}).

(**B9**) ^{1}H NMR (400 MHz, $CDCl_3$) δ 12.85 (s, 1H, OH), 8.74 (t, J = 2.1 Hz, 2H, CH_{ar}), 8.63 (d, J = 2.2 Hz, 2H, CH_{ar}), 8.37 (dd, J = 8.4, 2.3 Hz, 2H, CH_{ar}), 8.24 (d, J = 8.5 Hz, 1H, CH_{ar}), 8.07 (dd, J = 8.8, 2.2 Hz, 2H, CH_{ar}), 7.76 (t, J = 8.1 Hz, 2H, CH_{ar} and CH=CH), 7.13 (d, J = 8.8 Hz, 2H, CH_{ar} and CH=CH), and 2.67 (s, 6H, CH_3).

(**B10**) ^{1}H NMR (400 MHz, DMSO) δ 11.63 (s, 1H, OH), 8.82 (t, J = 2.1 Hz, 1H, CH_{ar}), 8.51 (d, J = 8.1 Hz, 1H, CH_{ar}), 8.46 (d, J = 2.2 Hz, 1H, CH_{ar}), 8.39 (dd, J = 8.0, 2.3 Hz, 1H, CH_{ar}), 8.30 (dd, J = 8.7, 2.3 Hz, 1H, CH_{ar}), 7.93–7.88 (m, 2H, CH_{ar} and CH=CH), 7.79 (d, J = 7.8 Hz, 2H, CH_{ar}),

TABLE III
THE FTIR SPECTRUM ASSIGNMENT FOR SYNTHESIS COMPOUNDS

Compound	str. Ar. C-N	str. C=O ketone or α, β ketone	str. C=C	str. C=C-H	str. Ar=C-H	str. sym. NO_2	str. asy. NO_2	C-H str. asy. (CH_3)	C-H ben. sym. (CH_3)	O-H str.	C-Cl str.
B1	1279	1681	1603	956	3067	1348	1530	2927	2861	3103	
B2	1288	1654, 1681	1593	971	3048	1347	1523			3089	
B3	1296	1664	1664	976	3063	1349	1527			3085	1049, 1075
B4	1296	1664	1614	977	3061	1349	1529			3086	1050, 1075
B5	1293	1663	1614	987	3082	1348	1527			3094	1042, 1072
B6	1270	1657	1600	975	3078	1345	1530			3100	Br 1075
B7	1276, 1288	1658	1599	977	3085	1348	1525			3099	Br 1093
B8	1275, 1287	1658	1600	977	3085	1347	1525			3099	1092
B9	1279	1681	1603	956	3068	1347	1530	2977	2865, 2872	3103	
B10	1281	1654	1654	981	3057	1345	1523	2924	2861	3103	
B11	1282	1658	1612	978	3079	1349	1522			3097	
B12	1279	1681	1603	956	3066	1347	1530			3103	

Ar. Aromatic, str. Stretching, bn. Bending. FTIR: Fourier-transform infrared spectroscopy

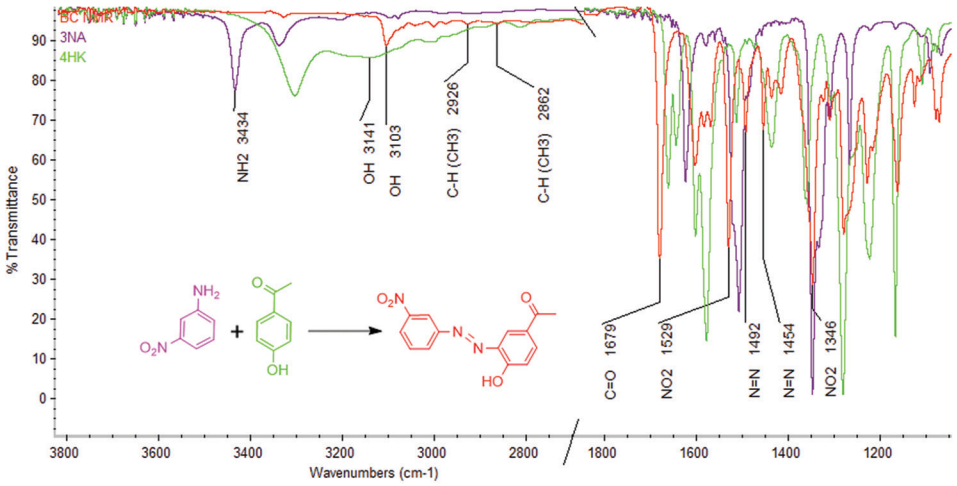

Fig. 6. Overlay of attenuated total reflectance spectrum of reactant and product **B1** compound.

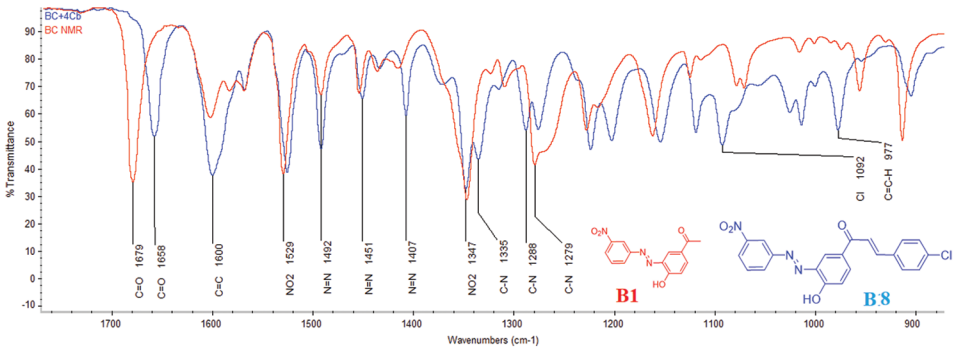

Fig. 7. Attenuated total reflectance overlay spectrum of compounds **B1** and **B8**.

7.72 (d, J = 15.6 Hz, 1H, CH=CH), 7.25 (dd, J = 14.0, 8.2 Hz, 3H, CH_{ar}), and 2.35 (s, 3H, CH_3).

(**B11**) ^{1}H NMR (400 MHz, $CDCl_3$) δ 12.90 (s, 1H, OH, CH_{ar}), 8.77 (t, J = 2.4 Hz, 1H, CH_{ar}), 8.73 (d, J = 2.4 Hz, 1H, CH_{ar}), 8.38 (ddd, J = 8.4, 2.4, 1.2 Hz, 1H, CH_{ar}), 8.25 (ddd, J = 8.0, 2, 1.2 Hz, 1H, CH_{ar}), 8.19 (dd, J = 8.8, 2.4 Hz, 1H, CH_{ar}), 7.90 (d, J = 15.6 Hz, 1H, CH=CH), 7.76 (t, J = 8.0 Hz, 1H, CH_{ar}), 7.74–7.7 (m, 2H, CH_{ar}), 7.65 (d, J = 15.6 Hz, 1H, CH=CH), 7.45–7.44 (m, 3H, CH_{ar}), and 7.18 (d, J = 8.8 Hz, 1H, CH_{ar}).

(**B12**) ^{1}H NMR (400 MHz, DMSO) δ 11.53 (s, 1H, OH), 8.72 (d, 3H, CH_{ar}), 8.59–8.18 (m, 5H, CH_{ar} and CH=CH), 8.11–7.76 (m, 3H, CH_{ar} and CH=CH), and 7.50–7.06 (m, 5H, CH_{ar} and CH=CH).

The following data illustrates ^{13}C NMR interpretation for synthesized compounds.

(**B1**) ^{13}C NMR (101 MHz, $CDCl_3$) δ 187.65 (C=O), 156.88 (C_{-OH}), 151.03 (C_{ar}), 149.38 (C_{ar}), 145.20 (C_{ar}), 144.31 (C_{ar}), 136.41 (C=C), 135.20 (C_{ar}), 134.93 (C_{ar}), 131.21 (C_{ar}), 130.86

http://dx.doi.org/10.14500/aro.11522

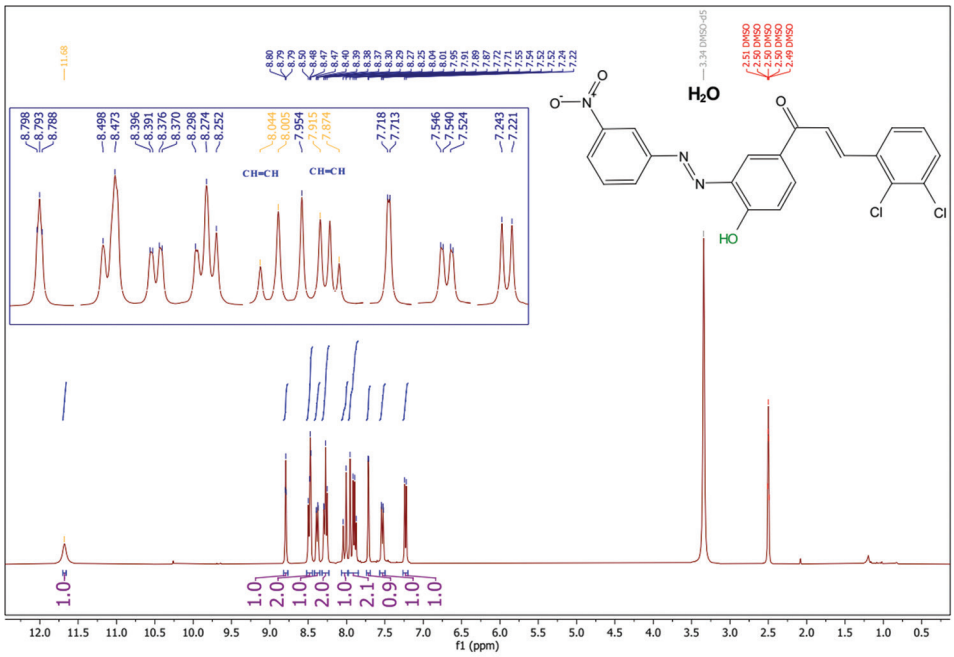

Fig. 8. ^{1}H NMR spectrum of synthesized azo chalcone product **B3**.

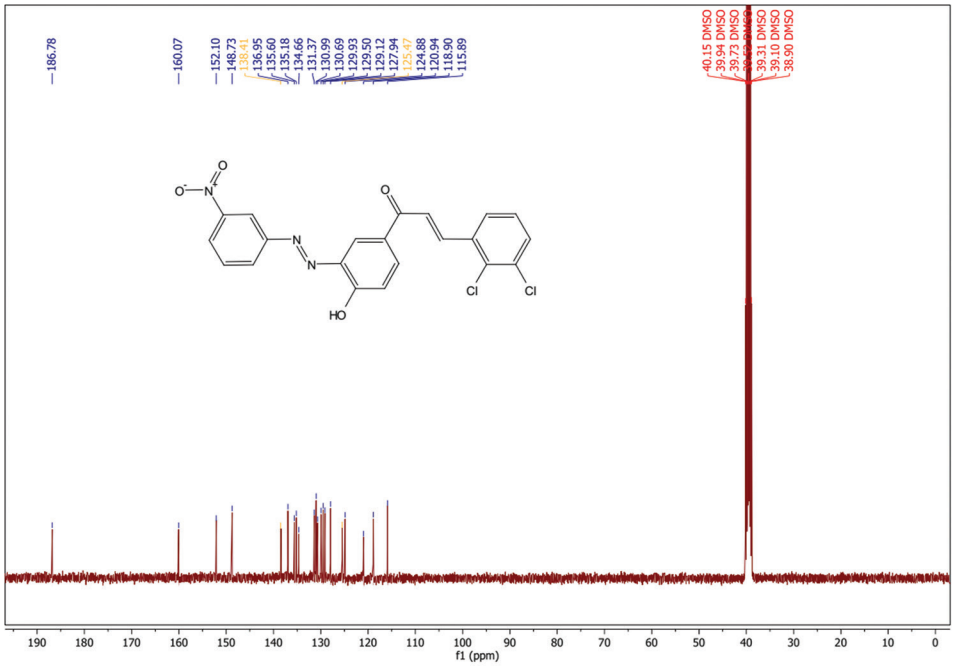

Fig. 9. ^{13}C NMR spectrum of synthesized azo chalcone product **B3**.

(C_{ar}), 130.65 (C_{ar}), 129.17 (2C_{ar}), 129.05 (C_{ar}), 128.72 (2C_{ar}), 125.69 (C=C), 121.06 (C_{ar}), 119.35 (C_{ar}), 116.50 (C_{ar}).

(**B2**) ^{13}C NMR (101 MHz, $CDCl_3$) δ 187.35 (C=O), 156.91 (C_{-OH}), 150.93 (C_{ar}), 149.29 (C_{ar}), 141.97 (C_{ar}), 136.38 (C=C), 135.26 (C_{ar}), 134.93 (C_{ar}), 133.86 (C_{ar}), 132.31 (C_{ar}), 131.91 (C_{ar}), 131.13 (C_{ar}), 130.59 (C_{ar}), 129.22 (C_{ar}), 128.94 (C_{ar}), 127.17 (C_{ar}), 126.48 (C_{ar}), 125.67 (C_{ar}), 125.61 (C=C), 125.29 (C_{ar}), 125.01 (C_{ar}), 123.58 (C_{ar}), 123.53 (C_{ar}), 119.37 (C_{ar}), 116.52 (C_{ar}).

(**B3**) ^{13}C NMR (101 MHz, DMSO) δ 186.78 (C=O), 160.07 (C_{-OH}), 152.10 (C_{ar}), 148.73 (C_{ar}), 138.41 (C=C), 136.95 (C_{ar}), 135.60 (C_{ar}), 135.18 (C_{ar}), 134.66 (C_{ar}), 131.37 (C_{ar}), 130.99 (C_{ar}), 130.69 (C_{ar}), 129.93 (C_{ar}), 129.50 (C_{ar}), 129.12 (C_{ar}), 127.94 (C_{ar}), 125.47 (C=C), 124.88 (C_{ar}), 120.94 (C_{ar}), 118.90 (C_{ar}), 115.89 (C_{ar}).

(**B4**) ^{13}C NMR (101 MHz, DMSO) δ 186.84 (C=O), 160.15 (C_{-OH}), 152.14 (C_{ar}), 148.76 (C_{ar}), 138.47 (C=C), 136.97 (C_{ar}), 135.62 (C_{ar}), 135.19 (C_{ar}), 134.68 (C_{ar}), 131.39 (C_{ar}), 131.02 (C_{ar}), 130.72 (C_{ar}), 129.96 (C_{ar}), 129.52 (C_{ar}), 129.11 (C_{ar}), 127.97 (C_{ar}), 125.48 (C=C), 124.95 (C_{ar}), 120.81 (C_{ar}), 118.94 (C_{ar}), 115.90 (C_{ar}).

(**B5**) ^{13}C NMR (101 MHz, DMSO) δ 187.21 (C=O), 160.49 (C_{-OH}), 152.53 (C_{ar}), 149.16 (C_{ar}), 138.84 (C=C),

137.38 (C_{ar}), 136.03 (C_{ar}), 135.61 (C_{ar}), 135.09 (C_{ar}), 131.80 (C_{ar}), 131.42 (C_{ar}), 131.12 (C_{ar}), 130.36 (C_{ar}), 129.93 (C_{ar}), 129.55 (C_{ar}), 128.37 (C_{ar}), 125.90 (C_{ar}), 125.31 (C=C), 121.37 (C_{ar}), 119.33 (C_{ar}), 116.32 (C_{ar}).

(**B6**) ^{13}C NMR (101 MHz, DMSO) δ 186.99 (C=O), 160.11 (C_{-OH}), 152.15 (C_{ar}), 148.75 (C_{ar}), 147.49 (C_{ar}), 141.00 (C_{ar}), 138.47 (C=C), 134.63 (C_{ar}), 134.00 (C_{ar}), 133.31 (C_{ar}), 132.15 (C_{ar}), 130.98 (C_{ar}), 130.70 (C_{ar}), 129.17 (C_{ar}), 128.88 (C_{ar}), 128.24 (C_{ar}), 125.43 (C=C), 124.59 (C_{ar}), 120.71 (C_{ar}), 118.94 (C_{ar}), 115.89 (C_{ar}).

(**B7**) ^{13}C NMR (101 MHz, DMSO) δ 187.06 (C=O), 159.91 (C_{-OH}), 152.14 (C_{ar}), 148.75 (C_{ar}), 142.28 (C_{ar}), 138.44 (C=C), 135.08 (C_{ar}), 134.59 (C_{ar}), 133.71 (C_{ar}), 130.98 (C_{ar}), 130.68 ($2C_{ar}$), 129.41 (C_{ar}), 128.96 ($2C_{ar}$), 125.44 (C=C), 122.39 (C_{ar}), 120.66 (C_{ar}), 118.83 (C_{ar}), 115.90 (C_{ar}).

(**B8**) ^{13}C NMR (101 MHz, DMSO) δ 187.10 (C=O), 159.92 (C_{-OH}), 157.14 (C_{ar}), 152.17 (C_{ar}), 148.76 (C_{ar}), 142.29 (C_{ar}), 138.48 (C=C), 138.15 (C_{ar}), 134.59 (C_{ar}), 133.70 (C_{ar}), 130.99 (C_{ar}), 130.68 ($2C_{ar}$), 129.41 (C_{ar}), 128.95 ($2C_{ar}$), 125.45 (C=C), 122.42 (C_{ar}), 120.53 (C_{ar}), 118.84 (C_{ar}), 115.90 (C_{ar}).

(**B9**) ^{13}C NMR (101 MHz, DMSO) δ 187.18 (C=O), 159.84 (C_{-OH}), 159.64 (C_{ar}), 152.11 (C_{ar}), 148.71 (C_{ar}), 143.74 (C_{ar}), 138.41 (C=C), 136.11 (C_{ar}), 134.60 (C_{ar}), 130.93 (C_{ar}), 130.69 (C_{ar}), 129.92 (C_{ar}), 129.48 (C_{ar}), 125.39 (C=C), 121.93 (C_{ar}), 121.64 (C_{ar}), 120.65 (C_{ar}), 118.76 (C_{ar}), 116.55 (C_{ar}), 115.86 (C_{ar}), 113.62 (C_{ar}), 55.31 (C_{ar}).

(**B10**) ^{13}C NMR (101 MHz, DMSO) δ 187.14 (C=O), 159.80 (C_{-OH}), 152.17 (C_{ar}), 148.75 (C_{ar}), 143.84 (C_{ar}), 140.69 (C_{ar}), 138.44 (C=C), 134.52 (C_{ar}), 132.01 (C_{ar}), 130.97 (C_{ar}), 130.69 (C_{ar}), 129.61 (C_{ar}), 129.56 ($2C_{ar}$), 129.01 ($2C_{ar}$), 125.41 (C=C), 120.59 (C_{ar}), 120.46 (C_{ar}), 118.80 (C_{ar}), 115.91 (C_{ar}), 21.15 (CH_3).

(**B11**) ^{13}C NMR (100.2 MHz, $CDCl_3$) δ 187.65 (C=O), 156.88 (C_{-OH}), 151.03 (C_{ar}), 149.38 (C_{ar}), 145.20 (C_{ar}), 144.31 (C_{ar}), 136.41 (C=C), 135.20 (C_{ar}), 134.93 (C_{ar}), 131.21 (C_{ar}), 130.86 (C_{ar}), 130.65 (C_{ar}), 129.17 (C_{ar}), 129.05 (C_{ar}), 128.72 ($2C_{ar}$), 125.69 (C=C), 121.06 (C_{ar}), 119.35 (C_{ar}), 116.50 (C_{ar}).

(B12) ^{13}C NMR (101 MHz, $CDCl_3$) δ 187.60 (C=O), 156.89 (C_{-OH}), 151.03 (C_{ar}), 145.30 (C_{ar}), 136.43 (C=C), 135.24 (C_{ar}), 134.97 (C_{ar}), 134.60 (C_{ar}), 133.50 (C_{ar}), 132.42 (C_{ar}), 131.29 (C_{ar}), 131.09 (C_{ar}), 130.66 (C_{ar}), 129.05 (C_{ar}), 128.96 (C_{ar}), 128.85 (C_{ar}), 127.98 (C_{ar}), 127.63 (C_{ar}), 126.98 (C=C), 125.71 (C=C), 123.82 (C_{ar}), 121.10 (C_{ar}), 119.38 (C_{ar}), 116.52 (C_{ar}).

C. Molecular Docking

Drug molecules' interactions with proteins can be seen using molecular docking. The goal of molecular docking calculations is to predict which mode of interaction between a given protein and ligand is most likely. These results are shown in Table II formerly known as C30 endopeptidase or 3-chymotrypsin-like protease, and the primary protease found in coronaviruses is referred to as 3C-like protease (3CLpro) or main protease (Mpro). It breaks down eleven conserved sites on the coronavirus polyprotein. It is a cysteine protease and a member of the PA clan of proteases. At its active site, it has a cysteine-histidine catalytic dyad that cleaves a Gln-(Ser/Ala/Gly) peptide bond (Ahmad, et al., 2021).

This family is known as the SARS coronavirus main proteinase, according to the Enzyme Commission. Nonstructural protein 5 (nsp5) of the coronavirus is correlated with the 3CL protease. The 3C protease (3Cpro), a homologous protease present in picornaviruses, is denoted by the letter "3C" in the common name. There are two hydrogen bonding (H. B.) links between compound **B2** and the protein. The two bonds link with the active sites THR 111 and HIS 246 of the protein. Compound **B3** forms only one H.B. link with the active site HIS246 of the protein. Compound **B4** interacts with the residues of the protein's active sites, GLN 110 and HIS 246 to form two linkages. Compound **B5** interacts with the residues of the protein's active sites, PRO108, THR 111, and HIS 246 to form three links, which are shown in Fig. 3a. These three interactions provide evidence of the higher activity of compound **B5** toward the protein. Compound **B6** is linked with the protein's active sites, ARG298 and ALA7 by two H. B. Compound **B7** linked with protein's active sites, GLN110 and HIS 246 through two H. B. Compound **B8** linked with protein's active sites, GLN110 and HIS 246 by two H. B. Fig. 3b. Compound **B9** forms two H. B. connections with the protein residues in their active sites GLN110 and HIS 246. Compound **B10** establishes three connections with the protein residues GLY15, GLY120, and GLY71 in the active site. These three interactions provide evidence of the higher activity of compound **B10** like compound **B5** toward the protein. Compound **B11** linked with protein's active sites, SER158, LYS102 by two H. B. Finally, the compound **B12** establishes three H. B. connections with the active site residues of proteins ASN 151, THR 111, and PRO 108. Furthermore, these three interactions provide evidence of the higher activity like compounds **B5** and **B10**. The results of molecular docking scores for synthesized compounds in Table II showed that the best compounds with higher binding ability were **B5** and **B8** because they had a high docking score (ΔG −6.235 kcal/mol) and (−5.832 kcal/mol), respectively (Mohamed, Mahmoud and Refaat, 2020). Although compound **B8** had two H. B.s, it shows a high docking score. It is worth mentioning that, compounds **B10** and **B12** each had three H. B.s with protein, but they showed lower activity than **B5** and **B8** due to the low docking scores (ΔG −5.654 kcal/mol) and (−5.364 kcal/mol) of **B10** and **B12,** respectively.

IV. Conclusion

The synthesis of novel azo and azo chalcones (**B1-B12**) was performed. All the synthesized compounds were completely identified by FTIR (ATR) and NMR. The ^{1}HNMR spectrum shows significant doublet peaks of the AB system at 8.18–7.3 ppm with J coupling at 15.60 Hz for all compounds except B2 and B6 at 15.20 Hz whereas ^{13}C NMR appears with two significant peaks at 136–145 and 125.41–125.93 ppm for two carbons of C=C. All these compounds were evaluated for

antiviral potential against SARS-CoV-2 3CL. Among them, compounds **B5** (ΔG −6.235 kcal/mol) and **B8** (ΔG −5.832 kcal/mol) showed more potential activity or binding ability toward the virus.

Acknowledgment

The author would like to appreciate Barcopharma Co. (agent of Thermo Fisher Co.) for their support that made this work easy and possible.

References

Abbas, S., Al-Hamdani, A.L.I., and Shaker, S.A., 2011. Synthesis, characterization, structural studies and biological activity of a new schiff base-Azo ligand and its complexation with selected metal ions. *Oriental Journal of Chemistry*, 27(3), pp.835-845.

Ahmad, B., Batool, M., Ul Ain, Q., Kim, M.S., and Choi, S., 2021. Exploring the binding mechanism of PF-07321332 SARS-CoV-2 protease inhibitor through molecular dynamics and binding free energy simulations. *International Journal of Molecular Sciences*, 22(17), p.9124.

Aksöz, B.E., and Ertan, R., 2012. Spectral properties of chalcones II. *Fabad Journal of Pharmaceutical Sciences*, 37(4), pp.205-216.

ALKazmi, A.A., Hawais, F.E., and Alasadi, Y.K., 2023. Synthesis and characterization of some pyrazoline derivatives from Chalcones containing azo and ether groups. *Tikrit Journal of Pure Science*, 22(9), pp.69-75.

Baper, S.H., and Mohammd, M.S., 2023. Synthesis, characterization and study anticancer activity of new Azo-Chalcone with mix Ligand of some divalent metal chelate complexes. *Journal of Kufa for Chemical Sciences*, 2(9), pp.390-408.

Benkhaya, S., M'rabet, S., and El Harfi, A., 2020. Classifications, properties, recent synthesis and applications of azo dyes. *Heliyon*, 6(1), p.e03271.

Botros, R., and CreeK, B., 1977. Azomethine dyes derived from an O-Hydroxy aromaticaldehyde and A 2-Amnopyrone', United State Patent 405119A. Available from: https://patentimages.storage.googleapis.com/aa/21/3e/16ceb20dd9212f/US4051119.pdf.

Calvino, V., Picallo, M., López-Peinado, A.J., Martín-Aranda, R.M., and Durán-Valle, C.J., 2005. Ultrasound accelerated Claisen-Schmidt condensation: A green route to chalcones. *Applied Surface Science*, 252(17), pp.6071-6074.

Chawsheen, M.A., and Al-Bustany, H.A., 2019. Docking study to predict the efficacy of phosphatidylinositol 3-kinase α inhibitors. *Aro-The Scientific Journal of Koya University*, 7(2), pp.47-52.

Clayden, J., Greeves, N., and Warren, S., 1995. Organic Chemistry. 2nd ed. Oxford University Press Inc., New York.

Elkanzi, N.A.A., Hrichi, H., Alolayan, R.A., Derafa, W., Zahou, F.M., and Bakr, R.B., 2022. Synthesis of chalcones derivatives and their biological activities: A review. *ACS Omega*, 7(32), pp.27769-27786.

Gür, M., 2019. Synthesis, characterization, and antimicrobial properties of new 1,3,4-thiadiazoles derived from azo dyes. *Journal of Heterocyclic Chemistry*, 56(3), pp.980-987.

Hawaiz, F.E., and Samad, M.K., 2012. Synthesis and spectroscopic characterization of some new biological active azo-pyrazoline derivatives. *European Journal of Chemistry*, 9(3), pp.1613-1622.

Hawaiz, F.E., Hussein, A.J., and Samad, M.K., 2014. One-pot three-component synthesis of some new azo-pyrazoline derivatives. *European Journal of Chemistry*, 5, pp.233-236.

Hawaiz, F.E., Samad, M.K., and Aziz, M.Y., 2015. Synthesis of some new heterocyclic compounds derived from 4-(4-hydroxy-3-chlorophenyl) azoaceto phenone. *Journal of Zankoy Sulaimani-Part A*, 17(2), pp.85-92.

Hsieh, C.T., Hsieh, T.J., El-Shazly, M., Chuang, D.W., Tsai, Y.H., Yen, C.T., Wu, S.F., Wu, Y.C., and Chang, F.R., 2012. Synthesis of chalcone derivatives as potential anti-diabetic agents. *Bioorganic and Medicinal Chemistry Letters*, 22(12), pp.3912-3915.

Hussein, A.J., and Aziz, H.J., 2011. Synthesis and spectroscopic characterization of some new azo-thiazolidinone derivatives. *Pelagia Research Library*, 2(5), pp.136-146.

Kadhium, A.J., Mohammed, M.S., and Baper, S.H., 2023. Design, preparation some transition metal complexes of Chalcone-Azo with Paracetamol ligand and Evaluation anti-biological activity of some complexes. *Journal of Kufa for Chemical Sciences*, 3(1), pp.55-67.

Kaka, K.N., Dabbagh, A.M., and Hamad, W.M., 2016. Kinetics study of the formation of pyrmidine thione from the reaction of 2,6-dibenzylidinecyclohexanone and its derivatives with thiourea. *ARO-The Scientific Journal of Koya University*, 4(2), pp.37-42.

Katritzky, A.R., Chen, Q.Y., and Tala, S.R., 2009. Convenient and efficient preparations of azodye-labeled peptides. *Chemical Biology and Drug Design*, 73(6), pp.611-617.

Kofie, W., Dzidzoramengor, C., and Adosraku, R.K., 2015. Synthesis and evaluation of antimicrobial properties of AZO dyes. *International Journal of Pharmacy and Pharmaceutical Sciences*, 7(4), pp.398-401.

Kozlowski, M.R., and Watson, A., 1992. Inhibition of gp120 binding to the CD4 antigen by dyes: Mechanism of effect and contribution to anti-HIV activity. *Antiviral Chemistry and Chemotherapy*, 3(1), pp.49-53.

Mamand, S.O., Abdul, D.A., Ayoob, M.A., Hussein, A.J., Samad, M.K., and Hawaiz, F.E., 2024. Traditional, one-pot three-component synthesis and anti-bacterial evaluations of some new pyrimidine derivatives. *Inorganic Chemistry Communications*, 160, p.111875.

Mezgebe, K., and Mulugeta, E., 2022. Synthesis and pharmacological activities of azo dye derivatives incorporating heterocyclic scaffolds: A review. *RSC Advances*, 12(40), pp.25932-25946.

Mohamed, G.G., Mahmoud, W.H., and Refaat, A.M., 2020. Nano-azo ligand and its superhydrophobic complexes: Synthesis, characterization, DFT, contact angle, molecular docking, and antimicrobial studies. *Journal of Chemistry*, 2020, pp. 19.

Okolo, E.N., Ugwu, D.I., Ezema, B.E., Ndefo, J.C., Eze, F.U., Ezema, C.G., Ezugwu, J.A., and Ujam, O.T., 2021. New chalcone derivatives as potential antimicrobial and antioxidant agent. *Scientific Reports*, 11(1), pp.1-13.

Pretsch, E., Bühlmann, P., and Badertscher, M., 2000. *Structure Determination of Organic Compounds: Table*

s of Spectral Data. Springer, Berlin.

Rohini, R.M., Devi, K., and Devi, S., 2015. Synthesis of novel phenyl azo chalcone derivatives for antitubercular, antiinflammatory and antioxidant activity. *Der Pharma Chemica*, 7(1), pp.77-83.

Shriner, R.L., Hermann, C.K.F., Morrill, T.C., Curtin, D.Y., and Fuson, R.C., 2004. *The Systematic Identification of Organic Compounds*. John Wiley & Sons. Inc., United States.

Sivasankerreddy, L., Nagamani, B., Rajkumar, T., Babu, M.S., Subbaiah, N.Y., Harika, M.S., and Nageswarao, R., 2018. Novel diazenyl containing phenyl styryl ketone derivatives as antimicrobial agents. *Anti-Infective Agents*, 17(1), pp.28-38.

Tawfiq, M.T., 2016. Synthesis and characterization of some new azo dyes derivatives via chalcone and study some of their biological activity. *Baghdad Science Journal*, 13(1), p.0122.

Vollheim, T., 1993. Survey of industrial chemistry. *Advanced Materials*, 5(5), p.400.

Yates, E., and Yates, A., 2016. Johann Peter Griess FRS (1829-88): Victorian brewer and synthetic dye chemist. *Notes and Records*, 70(1), pp.65-81.

Zweifel, G.S., Nantz, M.H., and Somfai, P., 2017. *Modern Organic Synthesis: An Introduction, Modern Organic Synthesis*. John Wiley & Sons, United States.